

## Coulomb interactions in carbon nanotubes

M. P. López Sancho,<sup>1</sup> M. C. Muñoz,<sup>1</sup> and L. Chico<sup>2</sup><sup>1</sup>*Instituto de Ciencia de Materiales de Madrid, Consejo Superior de Investigaciones Científicas, Cantoblanco, 28049 Madrid, Spain*  
<sup>2</sup>*Departamento de Física Aplicada, Facultad de Ciencias del Medio Ambiente, Universidad de Castilla-La Mancha, 45071 Toledo, Spain*

(Received 30 October 2000; published 4 April 2001)

The effect of electron-electron interactions on the electronic properties of nonchiral single-wall carbon nanotubes is investigated by an extended Hubbard model resolved within the generalized unrestricted Hartree-Fock approximation. On-site  $U$  and nearest-neighbor  $u$  Coulomb interactions are considered in tubules with different geometries at half-filling. A phase diagram is obtained in the coordinates  $U$  and  $u$ . For the electron-electron interaction strength estimated to hold for graphite, carbon nanotubes would lie close to the boundary region between metallic and insulator density wave states. Therefore, any small external perturbation can substantially modify their electronic properties.

DOI: 10.1103/PhysRevB.63.165419

PACS number(s): 73.21.-b, 71.20.Tx, 72.80.Rj

## I. INTRODUCTION

Carbon nanotubes (CNT's) constitute an interesting class of materials with fascinating properties. Since their discovery in 1991, a great amount of theoretical and experimental work has been dedicated to study different aspects of these quasi-one-dimensional (1D) materials.<sup>1</sup> Single-wall nanotubes (SWNT's) are created by rolling a graphene sheet into a cylindrical form. The tubule is usually characterized by two integers  $(n,m)$  specifying the circumference vector in an unrolled planar graphene sheet. Band-structure calculations<sup>2-5</sup> predict that the tubule geometry, which is given uniquely by the  $(n,m)$  indices, determines its electronic properties:  $(n,n)$  or armchair tubes are metals, while  $(n,0)$  or zigzag tubes are metals if  $n$  is a multiple of 3, or semiconductors otherwise. Chiral SWNT's  $(n,m)$  have electronic properties similar to zigzag tubes: if  $n-m$  is a multiple of 3, the tubules are metallic; otherwise, they are semiconducting. In all cases, the gap of the semiconducting tubes depends inversely on its radius.

As in other low-dimensional systems, electron-correlation effects are expected to become important for small nanotubes and have been theoretically explored from different points of view. Short-range (Hubbard-like) electron-electron interactions on armchair SWNT's at half-filling were considered<sup>6,7</sup> within a tight-binding description of the two gapless 1D bands crossing at the Fermi level and dispersing linearly. It was shown that, at half-filling, the low-energy theory of the  $(n,n)$  SWNT's is identical to a two-chain Hubbard model with an effective interaction  $u_n = U/n$ , which drives an instability to a Mott insulator with a gap in both charge and spin sectors.<sup>6</sup> Perturbative renormalization-group calculations<sup>7</sup> also show that electron-electron interactions change the metallic character of the  $(n,n)$  tubules into a Mott-insulating character with a spin gap. An effective low-energy theory, also for armchair nanotubes, was developed;<sup>8</sup> employing bosonization techniques in the strong-coupling regime, it was found that the Hamiltonian for an armchair SWNT is equivalent to that of two spin-1/2 fermion chains coupled by interactions but without interchain single-particle hopping, predicting ferromagnetic tendencies and a pseudogap behavior at very low temperatures.

Screened long-range Coulomb effects on armchair tubes with  $n \geq 10$  were also investigated in the framework of a Luttinger model.<sup>9</sup> Its inclusion results in significant deviations from the noninteracting behavior, thus converting the metallic tubes into strongly renormalized Luttinger liquids. From the microscopic lattice model, also by taking into account the screened long-range Coulomb interaction, the phase Hamiltonian for armchair NT's is derived<sup>10</sup> and, by renormalization-group techniques, it is found that at half-filling the ground state is a Mott insulator with a spin gap, in agreement with Hubbard-like models. Renormalization-group methods are used to study the low-energy behavior of the unscreened Coulomb interaction, which produces a strong renormalization of the Fermi velocity.<sup>11</sup> Finally, another interesting aspect theoretically explored is the interaction of CNT's in ropes: first-principles calculations predicted that interactions between armchair tubes in a rope induces a pseudogap of  $\approx 0.1$  eV at the Fermi level ( $E_F$ ).<sup>12</sup>

From an experimental point of view, some results present strong evidence of the remarkable dependence of the electronic properties on the geometry of the tubes, predicted by early band-structure calculations.<sup>2-5</sup> Scanning tunneling microscope (STM) experiments,<sup>13,14</sup> showed a direct relation between the atomic structure (diameter and helicity) and density of states of SWNT's. Armchair nanotubes were found to be metallic, with a finite density of states at  $E_F$  even at temperatures in the mK range. For semiconducting tubes, the linear dependence of the band gap on the nanotube diameter was also confirmed, the coefficient of proportionality experimentally found been in agreement with theoretical predictions. However, transport properties are not yet well understood. Experimental measurements of the temperature dependence of the resistivity, in ropes with mainly armchair tubes, reported a metallic behavior with an intrinsic resistivity which increases linearly with temperature.<sup>15,16</sup> Ferromagnetic correlations<sup>8</sup> have been invoked to explain electrical transport measurements on individual SWNT's.<sup>17</sup> On the other hand, transport spectroscopy experiments on a SWNT (Ref. 18) cannot be explained on the basis of independent-particle models. The data indicate a nontrivial shell-filling and spin polarization in carbon nanotubes, pointing to significant electron-electron correlations. This is in contrast

with previous transport spectroscopy results on a SWNT rope,<sup>19</sup> which fit the constant interaction model and showed no signatures of exotic electron correlations. Moreover, recent transport measurements at very low temperatures in SWNT's, which gave a conductance with a power-law behavior as a function of the temperature or bias voltage, were interpreted as a fingerprint of Luttinger-liquid behavior in metallic carbon nanotubes.<sup>20</sup> Such discrepancies might be due to the fact that transport experiments in nanotubes are difficult, and an interpretation of them is complex. Two- and four-probe contacts and bulk or end contacts give different results. The high contact resistances with leads observed may be due to the unique electronic structure of CNT's, which gives a weak electronic coupling at the Fermi surface; therefore, conduction between the CNT and metallic leads may be forbidden by Bloch symmetry.<sup>21</sup> Different factors such as structural distortions, thermal vibrations, and interaction with other tubules or the substrate affect electron transmission in the nanotube, posing an added difficulty to the interpretation of the experimental data. In fact, recently reported results have showed that the electronic properties of SWNT's are extremely sensitive to chemical environment,<sup>22</sup> indicating that many supposedly intrinsic properties measured on nanotubes may be due to gas adsorption on the large surface area of these materials. Since most experimental works use samples exposed to air, many measurements must be re-evaluated, taking into account the possible effects of gas adsorption on the electrical quantum conductance in CNT's.

In summary, in spite of the large amount of both theoretical and experimental work, an understanding of the CNT's properties is still lacking: many aspects of the physics of the nanotubes have no conclusive explanation, and the importance of electronic correlations is still an open question. In this work we examine the effects of Coulomb interactions on the electronic structure of armchair and zigzag tubules at half-filling, with an extended Hubbard Hamiltonian resolved within the unrestricted (or spin-polarized) Hartree-Fock approximation.

Although a mean-field approach, the unrestricted Hartree-Fock (UHF) approximation has turned out to be a powerful tool in the calculation of inhomogeneous states. Broken-symmetry states such as charge- or spin-density waves are stable solutions of the UHF theory. Along with the Hubbard model, it was used intensively in connection with 2D systems, especially in the study of electronic properties of cuprates and of the nickel and manganese oxide compounds.<sup>23</sup> Phase transitions were also widely investigated with Hartree-Fock (HF) theory:<sup>24,25</sup> although it is well known that the effect of quantum fluctuations could be important in critical behaviors, HF results yield a reasonably good qualitative picture. The importance of quantum fluctuations was pointed out in a quantum Monte Carlo finite-size scaling calculation for the nonmagnetic-semimetal to antiferromagnetic-insulator transition in a 2D honeycomb lattice, comparing with the corresponding transition in HF theory. Quantum fluctuations raise the HF critical value for the electronic interaction by a factor of 2, but the general behavior is correctly given within the Hartree-Fock scheme.<sup>25</sup>

The extended Hubbard model, along with the UHF ap-

proximation, was applied to graphite and graphite intercalation compounds<sup>26,27</sup> to analyze STM images, following Tersoff's idea<sup>28</sup> of the charge asymmetry on the two graphite sublattices. The truncated tetrahedron C<sub>12</sub> and icosahedron C<sub>60</sub> were also studied with the same model, and a magnetic-like instability of the Fermi sea toward a spin-ordered phase was found.<sup>29</sup> Nevertheless, this model has not been applied to CNT's. Such is the purpose of the present work.

The low-energy properties of undoped SWNT's differ from those away from half-filling, well described by Luttinger-like models,<sup>9,8,10</sup> due to umklapp scattering, which becomes the most relevant perturbation at half-filling.<sup>7,8</sup> In our model all scattering events are included, thus being appropriate for the study of both doped and undoped CNT's.

## II. MODEL AND METHOD

The Hubbard model describes itinerant electrons on a lattice interacting through on-site Coulomb repulsion.<sup>30</sup> The generalization of a Hubbard model that also includes nearest-neighbor interactions is known as the extended Hubbard model, defined by the Hamiltonian

$$\hat{H} = - \sum_{\langle ij \rangle, \sigma} t_{ij} c_{i\sigma}^\dagger c_{j\sigma} + U \sum_i n_{i\uparrow} n_{i\downarrow} + u \sum_{\langle i, j \rangle, \sigma, \sigma'} n_{i\sigma} n_{j\sigma'}, \quad (1)$$

where the operators  $c_{i\sigma}^\dagger (c_{j\sigma})$  creates (destroys) an electron of spin  $\sigma$  at site  $i$ ,  $n_{i\sigma} = c_{i\sigma}^\dagger c_{i\sigma}$  is the corresponding occupation number operator,  $t_{ij}$  represents the hopping integrals, and  $U$  and  $u$  stand for onsite and nearest-neighbor Coulomb interactions respectively. The symbol  $\langle ij \rangle$  denotes sum over nearest-neighbor sites. The calculation method was described extensively elsewhere,<sup>31</sup> so only the main features are outlined here. Upon linearization by standard mean-field techniques, the corresponding single-particle Hamiltonian describes the scattering in terms of the average local charges and bond orders. Charge and spin degrees of freedom are then calculated by a self-consistent procedure. As is generally accepted, a tight-binding model, with only one  $p_z$  orbital per carbon and a hopping matrix element  $t$  between neighboring atoms, correctly accounts for the low-energy physics of graphite and CNT's. Therefore, we restrict ourselves to the  $\pi$  electron of the carbon atom, taking the tight-binding (TB)  $\pi$ - $\pi$  nearest-neighbor hopping parameter for  $t_{ij}$  and neglecting curvature effects. The  $\pi$ - $\pi$  hopping integral reported in the literature ranges from 2.5 to 2.9 eV.<sup>13,16,32</sup> We use values between 2.66 and 2.70 eV, depending on the tube radius. Both on-site  $U$  and nearest-neighbor  $u$  Coulomb interactions are considered as parameters, varying between 0 and  $5t$  and  $2t$ , respectively, including the typical values for graphite. First, we study the effect of the on-site interaction  $U$ , setting  $u=0$ ; next, we look at the effect of  $u$  with  $U=0$ ; finally, we consider both on-site and intersite interactions simultaneously. For conjugated  $\pi$ -electron systems, detailed calculations have shown that as long as charge accumulation over large distances does not occur, the on-site and nearest-neighbor Coulomb repulsions are dominant.<sup>33</sup> Since

transport measurements have reported a high density of carriers in metallic CNT's,<sup>34</sup> it seems reasonable to retain only the terms  $U$  and  $u$ .

SWNT's are modeled by clusters consisting of  $N$  unit cells with periodic boundary conditions in order to minimize size effects. The unit cell (UC) is the corresponding ring of carbon atoms with the full symmetry and geometry of each tubule; both  $(n,n)$  and  $(n,0)$  nanotubes have  $4n$  atoms per UC. In order to investigate size effects, we considered different cluster sizes, and calculations were performed on clusters large enough as to obtain solutions with negligible size effects. To reach a self-consistent solution, around 50 iterations are sufficient in most cases; however, the number of iterations needed to obtain convergence increases considerably in the proximity of the critical values of the interactions.

As pointed out above, the ground state spin configuration of CNT's remains an open question,<sup>18,19</sup> and it is essential in the interpretation of the behavior of CNT electrons in external electric or magnetic fields. Since Coulomb repulsion between electrons affects states with different spin polarization in different ways, we considered three trial states: (i) an antiferromagnetic-like (AF) ordered state, where the average spin projection has opposite signs on adjacent sites; (ii) a uniform paramagnetic (PM) state, where charge and spin do not depend on the site; and (iii) a ferromagnetic (FM) state, with the same average spin projection in all sites.

In the AF trial state,  $\langle s_z \rangle = 0$  for all UC's and consequently the total spin is also 0. This state is assumed to be commensurate with the original bipartite lattice, with the symmetry of the  $C_3$  trigonal subgroup of the hexagonal group of the graphite plane. We have also considered the longitudinal AF state, where the average spin projection has opposite signs on adjacent UC's, but inside each UC all sites present the same average spin projection. This state is unstable, and always converges to a commensurate AF solution. In the PM state, as we are at the half-filling regime, the occupation is one per site, and  $s_z = 0$ . For intermediate values of the Coulomb interaction, such as the experimentally reported  $U$  between 6 and 10 eV for graphite,<sup>36</sup> the fully polarized ferromagnetic state is not a stable solution of the Hubbard model at half-filling. However, considering that electrical transport measurements under a magnetic field have been interpreted as indicative of ferromagnetic correlations,<sup>8,17</sup> we used the FM state as a trial function in order to investigate the possibility of ferromagnetic tendencies.

### III. RESULTS

#### A. Armchair tubules

Armchair  $(n,n)$  SWNT's are found to be metallic in band calculations for all  $n$ , because the set of allowed wave vectors always contains the  $\mathbf{K}$  points where the graphite bonding and antibonding bands cross at the Fermi level.<sup>3</sup> Here we present the results for (5,5) and (10,10) CNT's. These tubules have the same symmetry, the number of atoms per UC (40) and the radius ( $R = 6.781 \text{ \AA}$ ) of the (10,10) tube being twice those of the (5,5) tube. In both tubules, setting  $U = u = 0$ , the three initial states converge to the same final para-

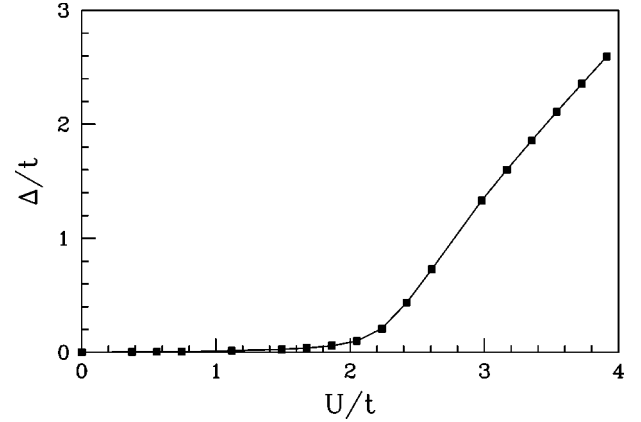


FIG. 1. Energy gaps as a function of the on-site Coulomb interaction corresponding to the self-consistent solutions obtained from the AF trial state for the armchair (5,5) NT.

magnetic solution, with the two bands crossing at  $\mathbf{K}$ . The one-electron densities of states (DOS's) present the expected spikes due to van Hove singularities, with small but finite DOS and a large separation between contiguous spikes around the Fermi energy ( $E_F$ ), in agreement with STM experiments and previous calculations.<sup>32</sup>

When the on-site Coulomb interaction  $U$  is switched on, the system undergoes a transition to an insulating phase beyond a critical value. This transition, driven by the on-site interaction, is characterized by the opening of a gap at the Fermi energy accompanied by an AF ordering of spins in which atoms of each sublattice have opposite spins. The (5,5) energy gap for the AF initial state as a function of the onsite Coulomb interaction is represented in Fig. 1. As is clearly seen, there is a change in the slope around  $U \approx 1.8t$ , and simultaneously there is an abrupt increase of  $\langle s_z \rangle$ . In the following,  $U_{c1}$ ,  $U_{c2}$ , and  $U_{c3}$  denote the critical  $U$  values for the AF, PM, and FM trial states, respectively. Since we are modeling CNT's by finite clusters, a vanishing small gap ( $\approx 0.002 \text{ eV}$ ) opens even below the critical values, due to finite-size effects. In fact, this small energy gap decreases as the number of cluster sites grows. Nevertheless, both the change of the slope and the enhancement of  $\langle s_z \rangle$  around  $U_{ci}$  do not present size effects for the cluster sizes considered here. Below  $U_{ci}$  the PM state converges to a PM solution, and the AF and FM trial states converge to solutions with weak AF and FM characters, respectively. The lowest critical value  $U_{c1}$  corresponds to the AF trial state, and the AF insulating solution presents the lowest energy. Above  $U_{c3}$  the three trial states converge to the same AF insulating solution. Both gap and spin polarizations gradually grow with  $U$ . This behavior is observed for both (5,5) and (10,10) tubules. The corresponding electronic band structure of the (5,5) CNT is depicted in Fig. 2(a) for  $U = 2.05t$ , showing the gap at  $E_F$ , where the two bands crossed at  $\mathbf{K}$  in the noninteracting case.

Next we investigate the effect of the nearest-neighbor repulsion, setting the on-site interaction  $U$  to 0 and switching on  $u$ . The behavior found for the gap and charge modulation versus  $u$  is similar to that found for the gap and spin ordering versus  $U$ . A change in the slope around  $u \approx 0.4t$ , with a simultaneous increase of the charge transfer from atoms of one

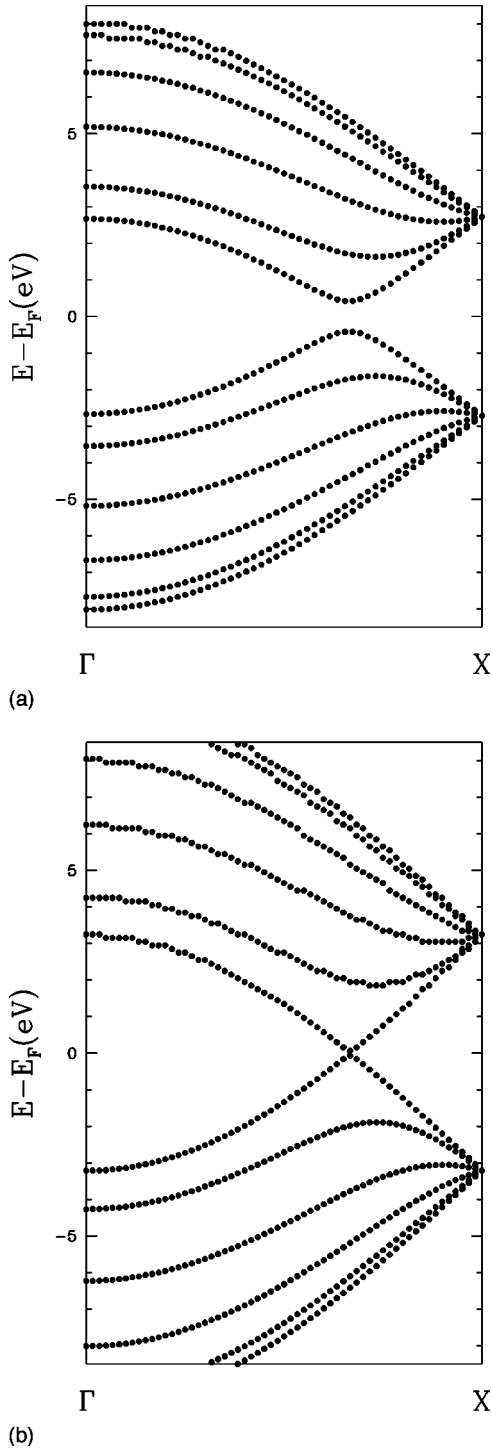


FIG. 2. Band structure for the (5,5) NT corresponding to (a) the SDW solution with a gap of 0.21 eV obtained for  $U=2.48t$  and  $u=0$ ; and (b) self-consistent solution obtained for  $U=2.23t$  and  $u=0.75t$ . Note the small gap of 0.05 eV.

sublattice to the other, indicates a transition.<sup>35</sup> The three trial states converge to the same insulating charge-ordered state, where the two carbon atoms of the graphite sublattices *A* and *B* carry different charges without spin polarization; they are commensurate charge-density-wave (CDW) states. Both the ordering of charges and the energy gap increase with  $u$ , and

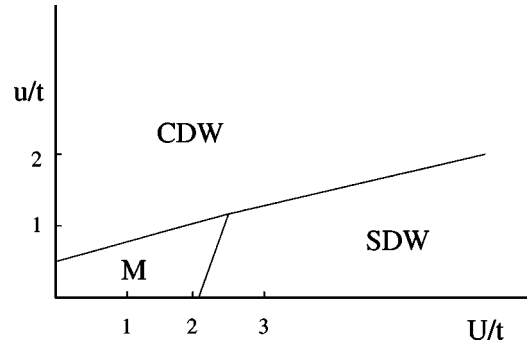


FIG. 3. Phase diagram of the (5,5) NT in the coordinates  $U/t$  and  $u/t$  obtained for a cluster of 30 UC's. The regions are labeled with the solution which presents the lowest energy.

for large enough  $u$  a state with alternating almost double and zero occupancies in the respective two sublattices is reached.

When both interactions are taken into account simultaneously, they compensate for each other in a range of values in which one of the interactions considered alone would have driven a transition to a gapped state. Figure 2(b) shows the band structure of the (5,5) NT with  $U$  and  $u$  higher than the critical values, illustrating this situation.

Taking into account both the on-site and intersite Coulomb repulsions, we obtain a phase diagram in the coordinates  $U$  and  $u$ , shown in Fig. 3. The regions are denoted with the character of the solution which presents the lowest energy. There exists a small region where  $U$  and  $u$  seem to cancel each other out, and the system converges to a metallic state. The system converges to the commensurate self-consistent spin-density-wave (SDW) solutions if  $U-3u>0$ , or CDW solutions if  $U-3u<0$ , as found for graphene.<sup>26</sup> The factor 3 is due to the coordination number of the graphite lattice. As SDW and CDW solutions are very close in energy around the line  $U=3u$ , convergence is very slow in the boundary region. The critical values  $U$  (setting  $u=0$ ) and  $u$  (setting  $U=0$ ), as well as the corresponding gaps and spin polarizations for the three initial states are indicated in Table I.

### B. Zigzag tubules

We next analyze the zigzag ( $n,0$ ) tubes. Without Coulomb interactions our calculations yield, as in the ( $n,n$ ) tubules, the behavior predicted in earlier TB and LDF calculations: semimetallic when  $n/3$  is an integer and semiconducting otherwise, with gaps depending on the tube diameter. The electronic band structure for (6,0), (7,0), and (9,0) CNT's calculated with  $U=u=0$  show that the (7,0) tubule is a semiconductor with an energy gap of 1.32 eV, while the (6,0) and (9,0) tubules are semimetals, in agreement with previous numerical studies.

The three initial states converge to the same final PM metallic solution for  $U=u=0$  in both (6,0) and (9,0) tubes. The behavior with increasing  $U$  is similar to that of the arm-chair tubes: above a certain  $U$  value, there is a change of the slope in the energy gap versus  $U$  curve, and in the spin

TABLE I. Critical values of the on-site  $U$  (with  $u=0$ ) and nearest-neighbor  $u$  (with  $U=0$ ) Coulomb interactions, in units of the hopping integral  $t$  for the three initial states considered in this work, are given for clusters of the armchair tubes (5,5) and (10,10), and of the zigzag tubes (6,0) and (9,0). Values of the corresponding gap  $\Delta$  (in eV) and spin polarization  $\langle s_z \rangle$  are also indicated.

	Initial st.	$U/t$	$\Delta$	$\langle s_z \rangle$	$u/t$	$\Delta$
(5,5)	AF	2.048	0.099	$\pm 0.049$	0.375	0.104
(5,5)	PM	2.234	0.242	$\pm 0.096$	0.375	0.103
(5,5)	FM	3.165	1.597	$\pm 0.379$	0.375	0.101
(10,10)	AF	2.060	0.096	$\pm 0.036$	0.375	0.077
(10,10)	PM	2.250	0.214	$\pm 0.087$	0.375	0.074
(10,10)	FM	3.195	1.604	$\pm 0.379$	0.375	0.076
(6,0)	AF	2.045	0.130	$\pm 0.04$	0.371	0.137
(6,0)	PM	2.230	0.272	$\pm 0.122$	0.371	0.138
(6,0)	FM	2.230	0.272	$\pm 0.092$	0.371	0.139
(9,0)	AF	2.050	0.126	$\pm 0.02$	0.374	0.099
(9,0)	PM	2.432	0.307	$\pm 0.132$	0.374	0.099
(9,0)	FM	2.432	0.743	$\pm 0.137$	0.374	0.086

polarization, such that the lowest energy solution is AF. For the AF spin-polarized initial state, the change in the slope takes place at  $U_{c1}$ , lower than the one needed for the PM and FM initial states, which converge to an insulating AF ordered solution at the same value  $U_{c2}=U_{c3}>U_{c1}$ . The gap and site spin projections increase with  $U$  in all cases, and, for  $U \geq U_{c1}$  the SDW solution always has the lowest energy. In Fig. 4 the band structure of the (9,0) NT corresponding to a SDW solution is depicted.

The CDW solutions appear when, setting  $U=0$ , the intersite correlation is switched on. In both (6,0) and (9,0) tubules

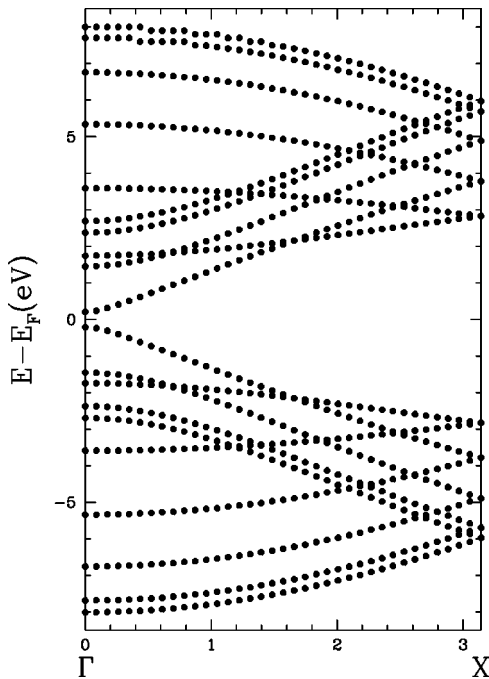


FIG. 4. Band structure for the zigzag (9,0) NT corresponding to a SDW solution obtained for  $U=1.87t$  and  $u=0$ .

the three trial states converge to an insulating CDW solution at the same critical  $u$ . Although the critical  $u$  are similar for both tubules, the associated gaps are different, being smaller for the larger tubule (see Table I). The electron densities in the atoms of the two sublattices  $A$  and  $B$  also present differences from the tube radius, being  $\langle n_A \rangle - \langle n_B \rangle = 0.124$  and  $0.088$  for the (6,0) and the (9,0) tubes respectively. In Table I critical values of  $U$  (setting  $u=0$ ) and  $u$  (setting  $U=0$ ) are shown for zigzag metallic tubules, as well as corresponding gaps and spin polarizations for the three initial states.

As stated above, the  $(n,0)$  tubules with  $n$  nonmultiple of 3 are already insulating without Coulomb interactions; therefore, the inclusion of  $U$  and  $u$  does not change their properties dramatically. In any case, we have studied the correlation effects on the (7,0) tubule, which has a gap of  $\Delta = 1.32$  eV for  $U=u=0$ . Starting with the AF trial state,  $U$  does not affect the gap appreciably up to  $U \approx 1.49t$ . Beyond this value the gap widens gradually, as expected. Considering the PM initial state, the gap decreases for  $t \leq U \leq 3.94t$  to  $\Delta = 0.743$  eV. Above this value the gap increases abruptly. For the FM initial state, an oscillatory decrease of the gap is found for  $2.62t \leq U \leq 4.12t$ ; above this value the gap enlarges. Conversely, with  $U=0$ , the effects of  $u$  on the three trial states are analogous: the gap increases gradually with  $u$ , and above  $\approx 1.3t$  the system converges to a charge-ordered state with almost double and zero occupancies. The phase diagram obtained for the  $(n,0)$  tubules is similar to that obtained for the  $(n,n)$  represented in Fig. 3.

When different values of the hopping integral  $t$  are adopted for the two bond orientations in both  $(n,0)$  NT's, even with  $U=u=0$  a small gap of the 0.058 and 0.026 eV opens on the (6,0) and (9,0) tubes, respectively, related to the gap induced by curvature effects. With increasing  $U$  and  $u$  the same general behavior is found. The (7,0) tube presents the same energy gap of 1.32 eV for  $U=u=0$ , considering one or two different hopping integrals.

#### IV. DISCUSSION

In summary, we have studied the role of on-site and nearest-neighbor Coulomb interactions on clusters with PBC modeling CNTs, at half-filling. In both metallic  $(n,n)$  and semi-metallic  $(n,0)$  interactions with  $n$  multiples of 3, we have found a metal-insulator Hubbard transition driven by Coulomb repulsion. The effects of the on-site Coulomb interaction on the electronic properties of  $(n,n)$  and  $(n,0)$  tubules at half-filling are similar. In both cases the system converges to a weakly AF spin-polarized state commensurate with the lattice, for  $U_c$  close but slightly lower than the one found for the graphene sheet. The gap opens smoothly, and gradually increases with the on-site Coulomb interaction  $U$ . A simultaneous onset of AF order is found at  $U=U_c$  which develops continuously as a function of  $U$ . From the opening of the gap this symmetry-broken SDW solution presents a lower energy than the homogeneous states. This gapped AF state is known as a Slater insulator.<sup>39</sup> When the effect of the intersite interaction  $u$  is analyzed, setting  $U=0$ , we find that, for the three initial states,  $u$  drives a transition to a gapped CDW state without spin polarization. The ordering of

charges (charge transfer from one sublattice to the other) and the gap grow with increasing  $u$ . Such a convergence to a CDW insulator state, with the same symmetry as the structural arrangement, is obtained for all  $(n,n)$  and  $(n,0)$  tubes considered.

Considering both on-site and intersite Coulomb repulsions, there exists a small region where the lowest-energy solution would present a metallic behavior, because  $U$  and  $u$  compensate for each other and the effective resulting interaction does not suffice to drive the transition to the gapped ordered phases. Two other regions exist depending on the  $U/u$  ratio, where the system converges to SDW and CDW insulating states, respectively. The SDW and CDW regions are divided by a narrow boundary region around the line  $U = 3u$ ; for  $U \geq 3u$  the SDW state presents the lowest energy, while for  $U \leq 3u$  the CDW solution is most favorable. The effects of the Coulomb interaction are very similar for all armchair and metallic zigzag tubes, and close to that of the graphene sheet, reflecting the underlying  $C_3$  symmetry of these systems. In fact, the complex nature of SWNT's, which present a large surface area, with the reduced symmetry of a single layer and a hollow geometry, may be responsible for their observed deviation from a pure 1D behavior. Taking into account that the critical values we have obtained in a mean field approach would be increased when considering quantum fluctuations, the region where the tubule behavior is metallic or semimetallic would be, at this energy range, non-negligible.

In the range of parameters estimated for a graphite layer,<sup>26,36</sup> both  $(n,n)$  and  $(n,0)$ , with  $n/3$  integer tubules, are close to the boundary between the metallic and insulating regions. These results are consistent with those obtained by the renormalization-group approach for armchair NT's: at half-filling the ground state is a Mott insulator with an exponentially small gap, in which bound states of electrons are formed at different atomic sublattices.<sup>9,10</sup> Due to the proximity to the boundary region, small variations of  $U$  or  $u$  may produce a crossover from one region to other. Consequently, small external perturbations (interaction with other tubes, substrate irregularities, external magnetic fields, etc.), which within this model can be taken into account by changing the Hamiltonian parameters, could substantially modify some of the fundamental electronic properties of the tubules.

Our results are compatible with a variety of experimental

signatures of the carbon nanotubes. A possible interpretation of the asymmetry in the STM images of CNT's is the appearance of a CDW, as pointed out previously<sup>37,38</sup> and corroborated by our calculations. Nevertheless, as the interpretation of the atomic lattice configuration observed in STM images is nontrivial, it could be possible that the last atom of the tip has a magnetic moment, thus the SDW could be the origin of the broken-symmetry patterns in the STM images. It was also reported recently that the electronic properties of CNT's are extremely sensitive to the chemical environment:<sup>22</sup> SWNTs showed a metallic behavior when exposed to air, but their transport properties changed significantly in vacuum. Then it might be possible that small gaps produced by electron-electron interactions were masked by the presence of adsorbed oxygen in the nanotubes, which could be doped due to such a contamination.

## V. CONCLUSIONS

Here we have studied the  $\pi$ -electron bands of CNT's by an extended Hubbard Hamiltonian at half-filling. The competition between the kinetic energy of the carriers and the Coulomb repulsion drives a transition between a homogeneous state and a gapped periodic ordering of charge and spin: the phase diagram in the  $U-u$  plane shows a small region where a metallic or semimetallic phase holds, and two regions where CDW and SDW insulating phases exist due to the interplay of  $U$  and  $u$ . In the range of estimations of the parameters for graphite, both  $(n,n)$  and  $(n,0)$  metallic tubules are on the insulating region, close to the boundary with the metallic zone; therefore, small variations of  $U$  or  $u$  may produce a transition to a metallic state or between SDW and CDW insulating states. These symmetry-broken solutions could be an explanation for the patterns observed in STM images of SWNT's. Small external perturbations could substantially modify some of the fundamental electronic properties of the tubules, as recently claimed by in an experiment.<sup>22</sup>

## ACKNOWLEDGMENTS

This work was partially supported by the Spanish MEC through DGICYT Grant Nos. PB98-0523 and PB96-0916, and by CAM (Madrid) through Grant Nos. 07/0045/98 and 07/0042/98. M.P.L.S. acknowledges useful discussions with Professor F. Guinea and Professor J. Rubio.

<sup>1</sup>T. Ebbesen, Phys. Today **49**(6), 26 (1996).

<sup>2</sup>R. Saito, M. Fujita, G. Dresselhaus, and M. S. Dresselhaus, Appl. Phys. Lett. **60**, 2204 (1992).

<sup>3</sup>N. Hamada, S. I. Sawada, and A. Oshiyama, Phys. Rev. Lett. **68**, 1579 (1992).

<sup>4</sup>J. W. Mintmire, B. I. Dunlap, and C. T. White, Phys. Rev. Lett. **68**, 631 (1992).

<sup>5</sup>C. L. Kane and E. J. Mele, Phys. Rev. Lett. **78**, 1932 (1997).

<sup>6</sup>L. Balents and M. P. A. Fisher, Phys. Rev. B **55**, R11 973 (1997).

<sup>7</sup>Y. A. Krotov, D.-H. Lee, and S. G. Louie, Phys. Rev. Lett. **78**, 4245 (1997).

<sup>8</sup>R. Egger and A. O. Gogolin, Phys. Rev. Lett. **79**, 5082 (1997).

<sup>9</sup>C. Kane, L. Balents, and M. P. A. Fisher, Phys. Rev. Lett. **79**, 5086 (1997).

<sup>10</sup>H. Yoshioka and A. A. Odintsov, Phys. Rev. Lett. **82**, 374 (1999).

<sup>11</sup>S. Bellucci and J. González, Eur. Phys. J. B (to be published).

<sup>12</sup>P. Delaney, H. J. Coi, J. Ihm, S. G. Louie, and M. L. Cohen, Nature (London) **391**, 466 (1998).

<sup>13</sup>J. W. C. Wildöer, L. C. Venema, A. G. Rinzler, R. E. Smalley, and C. Dekker, Nature (London) **391**, 59 (1998).

<sup>14</sup>T. W. Odom, J. L. Huang, P. Kim, and C. M. Lieber, Nature (London) **391**, 62 (1998).

- <sup>15</sup>J. E. Fischer, H. Dai, A. Thess, R. Lee, N. M. Hanjani, D. L. Dehaas, and R. E. Smalley, *Phys. Rev. B* **55**, R4921 (1997).
- <sup>16</sup>H. Kane, E. J. Mele, R. S. Lee, J. E. Fisher, P. Petit, H. Dai, A. Thess, R. E. Smalley, A. R. M. Verschuere, S. J. Tans, and C. Dekker, *Europhys. Lett.* **44**, 518 (1998).
- <sup>17</sup>S. J. Tans, M. H. Devoret, H. Dai, A. Thess, R. E. Smalley, L. J. Geerligs, and C. Dekker, *Nature (London)* **386**, 474 (1997).
- <sup>18</sup>S. J. Tans, M. H. Devoret, R. J. A. Groeneveld, and C. Dekker, *Nature (London)* **394**, 761 (1998).
- <sup>19</sup>D. H. Cobden, M. Bockrath, P. L. McEuen, A. G. Rinzler, and R. E. Smalley, *Phys. Rev. Lett.* **81**, 681 (1998).
- <sup>20</sup>M. Bockrath, D. H. Cobden, J. Lu, A. G. Rinzler, R. E. Smalley, L. Balents, and P. L. McEuen, *Nature (London)* **397**, 598 (1999).
- <sup>21</sup>J. Tersoff, *Appl. Phys. Lett.* **74**, 2122 (1999).
- <sup>22</sup>P. G. Collins, K. Bradley, M. Ishigami, and A. Zettl, *Science* **287**, 1801 (2000).
- <sup>23</sup>B. Goss-Levi, *Phys. Today* **51(6)**, 19 (1998), and references therein.
- <sup>24</sup>G. Santoro, S. Sorella, F. Becca, S. Scandolo, and E. Tosatti, *Surf. Sci.* **402-404**, 802 (1998).
- <sup>25</sup>S. Sorella and E. Tosatti, *Europhys. Lett.* **19**, 699 (1992).
- <sup>26</sup>A. L. Tchougreef and R. Hoffman, *J. Phys. Chem.* **96**, 8993 (1992).
- <sup>27</sup>F. R. Wagner and M. B. Lepetit, *J. Phys. Chem.* **100**, 11 050 (1996).
- <sup>28</sup>J. Tersoff, *Phys. Rev. Lett.* **57**, 440 (1986).
- <sup>29</sup>L. Bergomi, J. P. Blaizot, Th. Jolicœur, and E. Dagotto, *Phys. Rev. B* **47**, 5539 (1993).
- <sup>30</sup>J. Hubbard, *Proc. R. Soc. London, Ser. A* **276**, 238 (1963).
- <sup>31</sup>M. P. López Sancho, J. Rubio, M. C. Refolio, and J. M. López Sancho, *Phys. Rev. B* **46**, 11 110 (1992); **49**, 9125 (1994).
- <sup>32</sup>P. Kim, T. W. Odom, J. H. Huang, and C. M. Lieber, *Phys. Rev. Lett.* **82**, 1225 (1999).
- <sup>33</sup>D. Baeriswyl and E. Jeckelmann, in *The Hubbard Model*, edited by D. Baeriswyl *et al.* (Plenum Press, New York, 1995), p. 393.
- <sup>34</sup>Z. Yao, C. L. Kane, and C. Dekker, *Phys. Rev. Lett.* **84**, 2941 (2000).
- <sup>35</sup>As an example, for the (5,5) tube the difference in the charge populations of both sublattices goes from  $\langle n_A \rangle - \langle n_B \rangle = 0.084$  electron/atom when  $u = 0.375t$ , to 0.956 electron/atom if  $u = 0.55t$ . These values depend on the tube size; for the (10,10) tube,  $\langle n_A \rangle - \langle n_B \rangle$  changes from 0.070 to 0.890 electron/atom when varying the intersite repulsion from  $0.375t$  to  $0.55t$ .
- <sup>36</sup>R. G. Pearson, *Inorg. Chem.* **27**, 734 (1988).
- <sup>37</sup>C. L. Kane and E. J. Mele, *Phys. Rev. B* **59**, R12 759 (1999).
- <sup>38</sup>L. C. Venema, J. W. G. Wildöer, C. Dekker, G. Rinzler, and R. E. Smalley, *Appl. Phys. A: Mater. Sci. Process.* **66**, S153 (1998).
- <sup>39</sup>F. Gebhart, in *The Mott Metal-Insulator Transition*, edited by J. Khn *et al.*, Springer Tracts in Modern Physics Vol. 137 (Springer-Verlag, Berlin, 1997).